

## Doctor-bladed $\text{Cu}_2\text{ZnSnS}_4$ light absorption layer for low-cost solar cell application

This content has been downloaded from IOPscience. Please scroll down to see the full text.

2012 Chinese Phys. B 21 038401

(<http://iopscience.iop.org/1674-1056/21/3/038401>)

View [the table of contents for this issue](#), or go to the [journal homepage](#) for more

Download details:

IP Address: 202.120.209.10

This content was downloaded on 29/03/2017 at 06:38

Please note that [terms and conditions apply](#).

You may also be interested in:

[Solution-processed  \$\text{Cu}\_2\text{ZnSnS}\_4\$  superstrate solar cell using vertically aligned ZnO nanorods](#)

Dongwook Lee and Kijung Yong

[Printed ethyl cellulose/ \$\text{CuInSe}\_2\$  composite light absorber layer and its photovoltaic effect](#)

Qinmiao Chen, Xiaoming Dou, Zhenqing Li et al.

# Doctor-bladed $\text{Cu}_2\text{ZnSnS}_4$ light absorption layer for low-cost solar cell application

Chen Qin-Miao(陈勤妙)<sup>a)b)</sup>, Li Zhen-Qing(李振庆)<sup>a)b)</sup>, Ni Yi(倪一)<sup>b)</sup>, Cheng Shu-Yi(程抒一)<sup>b)</sup>,  
and Dou Xiao-Ming(窦晓鸣)<sup>a)b)c)†</sup>

<sup>a)</sup>Department of Physics, Shanghai Jiao Tong University, Shanghai 200240, China

<sup>b)</sup>School of Optical-Electrical and Computer Engineering, University of Shanghai for Science and Technology, Shanghai 200093, China

<sup>c)</sup>Consolidated Research Institute for Advanced Science and Medical Care, Waseda University, 513 Wasedatsurumaki-cho, Shinjuku-ku, Tokyo 162-0041, Japan

(Received 29 April 2011; revised manuscript received 23 October 2011)

The doctor-blade method is investigated for the preparation of  $\text{Cu}_2\text{ZnSnS}_4$  films for low-cost solar cell application.  $\text{Cu}_2\text{ZnSnS}_4$  precursor powder, the main raw material for the doctor-blade paste, is synthesized by a simple ball-milling process. The doctor-bladed  $\text{Cu}_2\text{ZnSnS}_4$  films are annealed in  $\text{N}_2$  ambient under various conditions and characterized by X-ray diffraction, ultraviolet/vis spectrophotometry, scanning electron microscopy, and current-voltage ( $J$ - $V$ ) measurement. Our experimental results indicate that (i) the X-ray diffraction peaks of the  $\text{Cu}_2\text{ZnSnS}_4$  precursor powder each show a red shift of about  $0.4^\circ$ ; (ii) the high-temperature annealing process can effectively improve the crystallinity of the doctor-bladed  $\text{Cu}_2\text{ZnSnS}_4$ , whereas an overlong annealing introduces defects; (iii) the band gap value of the doctor-bladed  $\text{Cu}_2\text{ZnSnS}_4$  is around 1.41 eV; (iv) the short-circuit current density, the open-circuit voltage, the fill factor, and the efficiency of the best  $\text{Cu}_2\text{ZnSnS}_4$  solar cell obtained with the superstrate structure of fluorine-doped tin oxide glass/ $\text{TiO}_2/\text{In}_2\text{S}_3/\text{Cu}_2\text{ZnSnS}_4/\text{Mo}$  are  $7.82 \text{ mA/cm}^2$ , 240 mV, 0.29, and 0.55%, respectively.

**Keywords:**  $\text{Cu}_2\text{ZnSnS}_4$ , non-vacuum process, mechanochemical ball-milling process, doctor-blade method

**PACS:** 84.60.Jt, 88.40.H-, 88.40.hm

**DOI:** 10.1088/1674-1056/21/3/038401

## 1. Introduction

A number of different types of materials, such as silicon,<sup>[1,2]</sup> inorganic compounds, and polymer,<sup>[3,4]</sup> have been used for constructing solar cells. Among them, the inorganic compound  $\text{CuIn}_x\text{Ga}_{1-x}\text{Se}_2$  (CIGS) has been intensively investigated as a promising absorption layer material for low-cost solar cell application.<sup>[5-7]</sup> However, the constituent elements of CIGS are expensive (In and Ga) and toxic (Se). In searching for a chalcopyrite photovoltaic absorption layer material with nontoxic or less toxic elements,  $\text{Cu}_2\text{ZnSnS}_4$  (CZTS) has emerged as the most promising material. It has a near-optimal direct band gap of about 1.5 eV and a larger absorption coefficient ( $>10^4/\text{cm}$ ).<sup>[8-10]</sup> Moreover, the CZTS is nontoxic, and its elements are abundant in the Earth's crust. The conventional structure of the CZTS solar cell is glass/Mo/CZTS/CdS/ZnO/ZnO:Al/Al, which is called the substrate structure, and the quaternary

CZTS absorption layer is prepared by using vacuum methods.<sup>[8-16]</sup> Katagiri *et al.*<sup>[8]</sup> reported a CZTS solar cell with a conversion efficiency of 6.77%, in which the CZTS absorption layer was deposited by a three-source co-sputtering process. However, the vacuum fabrication processes are rather expensive, complicated, and difficult to scale-up for commercial production.

Recently, many non-vacuum processes, such as printing,<sup>[17-24]</sup> spray pyrolysis,<sup>[25,26]</sup> and electrochemical deposition technology,<sup>[27]</sup> have sprung up for preparing low-cost solar cells. Todorov *et al.*<sup>[17]</sup> reported a 9.66% conversion efficiency CZTSSe solar cell, in which the CZTSSe absorption layer was prepared by a hydrazine (high-toxic) based spin-coating process. Zhou *et al.*<sup>[19]</sup> demonstrated a CZTS solar cell with a conversion efficiency of 0.49%, in which the CZTS absorption layer was deposited by using screen-printing technology and the CZTS precursor powder was synthesized by a simple ball-milling process.<sup>[28,29]</sup>

<sup>†</sup>Corresponding author. E-mail: xm.dou@yahoo.com.cn

These results indicate that printing technology, such as the above-mentioned spin coating and screen printing, could lead to a possible cost reduction for solar cell production. In addition, the doctor-blade is also an attractive printing technology, because it is widely used for large area film production and has some additional advantages. (i) The material utilization is close to 100%. Spin coating is employed mainly for thin films with small areas and may result in high losses of materials. (ii) The preparation process is simple. For screen printing, an organic dispersion agent is usually used to prepare the paste, and consequently the organic agent may partly reside as a residue in the resulting semiconductor device. Therefore, the doctor-blade technology could be an alternative process for preparing CZTS films for low-cost solar cells. However, to the best of our knowledge, until now there has been no report on the preparation of CZTS film by using the doctor-blade method.

In this work, we develop a solar cell with the substrate structure of fluorine-doped tin oxide (FTO) glass/TiO<sub>2</sub>/In<sub>2</sub>S<sub>3</sub>/CZTS/Mo, and the CZTS absorption layer is prepared by using the doctor-blade technology. In addition, In<sub>2</sub>S<sub>3</sub> is chosen as the buffer layer for the solar cell instead of the conventionally used high-toxic CdS buffer layer. Both the compact TiO<sub>2</sub> window layer and the In<sub>2</sub>S<sub>3</sub> buffer layer are prepared by using the non-vacuum spray pyrolysis method to further simplify the preparation processes and to reduce the entire production cost. We investigate the annealing effects on the properties of the doctor-bladed CZTS film by X-ray diffraction (XRD), ultraviolet/vis spectrophotometry (UV), scanning electron microscopy (SEM), and current–voltage (*J–V*) measurement.

## 2. Experimental details

### 2.1. Preparation of the CZTS films

For analyzing the annealing effects on the properties of the doctor-bladed CZTS, the CZTS paste was doctor-bladed on the glass substrates. The obtained samples were referred to as CZTS films. The detailed preparation process of the CZTS films is described as follows.

#### 2.1.1. Synthesis of the CZTS precursor powder

The ball-milling process was adopted for the synthesis of the CZTS precursor powder. Element

powders Cu (99.9%, Wako Chemicals), Zn (99.9%, Wako Chemicals), Sn (99.5%, Aldrich), and S (99.9%, Kishida Chemicals) were mixed in molar ratio 2:1:1:4. The mechanochemical ball-milling process was conducted in a planetary ball miller (M2-3F, Gokin) at various rotation speeds to obtain good CZTS precursor powders. The experimental condition of (800 rpm, 1 h) was optimum to obtain the single phase CZTS precursor powder.

#### 2.1.2. Preparation of the CZTS paste

The CZTS paste was prepared in a milling motor using the following steps. (i) The CZTS precursor powder was first ground alone for about 5 min. (ii) Then 1 ml 10 wt.% thiourea aqueous solution (Kishida Chemicals) was slowly added while keeping grinding for about 10 min. (iii) Finally, 2 ml propylene glycol (Kando chemicals) was slowly added while keeping grinding for another 10 min. The milling duration for each step may be slightly changed to obtain doctor-blade pastes with desirable viscosity.

#### 2.1.3. Deposition of the CZTS films

The CZTS paste was deposited on the glass substrates using the doctor-blade method. After drying treatment at 125 °C for 5 min in air (the dried sample will be called the as-deposited sample), the samples were processed by rapid thermal annealing (RTA) in N<sub>2</sub> ambient under various conditions. The annealed films were characterized by XRD, UV, SEM, and *J–V*.

## 2.2. Fabrication of the CZTS solar cell

The structure of the solar cell is depicted in Fig. 1, and a flow diagram of the solar cell fabrication process is shown in Fig. 2. The corresponding thin film layers of the solar cell were prepared as follows.

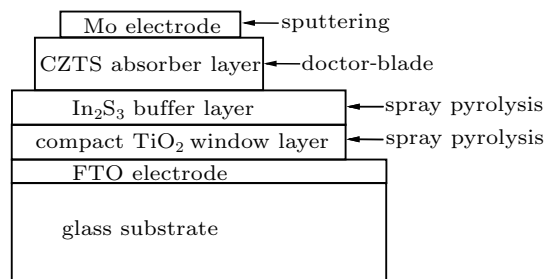


Fig. 1. Structure of the solar cell.

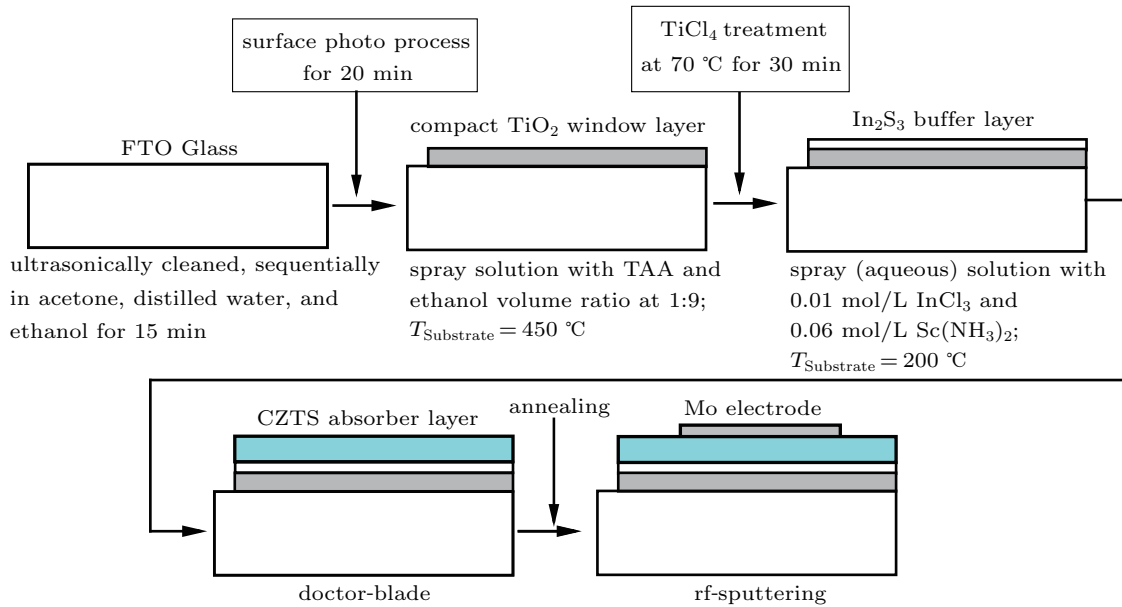


Fig. 2. Flow diagram of the solar cell fabrication process.

### 2.2.1. Deposition of compact TiO<sub>2</sub> window layer and In<sub>2</sub>S<sub>3</sub> buffer layer

Both compact TiO<sub>2</sub> window layer and In<sub>2</sub>S<sub>3</sub> buffer layer were prepared by using the spray pyrolysis method.<sup>[30,31]</sup>

For the compact TiO<sub>2</sub> window layer, titanium isopropoxide (99%, Kishida Chemicals) and acetylacetone (99.5%, Wako Chemicals) were mixed with a molar ratio of 0.5 (TAA). The mixture solution was further diluted by ethanol (TAA:ethanol = 1:9 (v/v)) to make a spray solution. Prior to spraying, the FTO glass substrate (10 cm × 10 cm) was cleaned in ultrasonic solutions of acetone, distilled water, and ethanol sequentially for 15 min each, and the dried sample was treated by a UV/O<sub>3</sub> cleaner (PL16-110, Sen Lights Corporation) for 20 min to remove organic dust from the FTO surface. The substrate temperature was kept at 450 °C during spraying, and a 50 ml spray solution was employed for the compact TiO<sub>2</sub> window layer deposition.

For the In<sub>2</sub>S<sub>3</sub> buffer layer, 50 mL aqueous solution with 0.01 mol/L InCl<sub>3</sub> (98%, Tokyo Chemicals, anhydrous) and 0.06 mol/L thiourea was employed, additional thiourea was intentionally used to create a sulfur-rich buffer layer. The CZTS absorption layer was grown on the buffer layer, thus the sulfur-rich buffer layer could benefit the quality improvement of the CZTS absorption layer during annealing. Before the In<sub>2</sub>S<sub>3</sub> buffer layer was sprayed, the compact TiO<sub>2</sub> window layer was treated with 40 mmol/L TiCl<sub>4</sub> aqueous solution (1.50–1.69 mg/ml, Wako Chemicals) at

70 °C for 30 min to smooth the film. The substrate temperature of the buffer layer spray was 200 °C.

The thicknesses of the deposited compact TiO<sub>2</sub> window layer and the In<sub>2</sub>S<sub>3</sub> buffer layer were about 100 nm and 300 nm, respectively.

### 2.2.2. Fabrication of CZTS solar cell

The CZTS paste was doctor-bladed on the prepared FTO glass/TiO<sub>2</sub>/In<sub>2</sub>S<sub>3</sub> substrates. The obtained samples (FTO glass/TiO<sub>2</sub>/In<sub>2</sub>S<sub>3</sub>/CZTS) were annealed by using the RTA process in N<sub>2</sub> ambient under different conditions. Finally, Mo electrodes were sputtered on the annealed samples to complete the CZTS solar cells fabrication (FTO glass/TiO<sub>2</sub>/In<sub>2</sub>S<sub>3</sub>/CZTS/Mo). The active area of the solar cell was 0.5 cm × 0.5 cm.

### 2.3. Characterization method

The crystallinity and the phase composition of the CZTS films were confirmed by XRD (MiniFlex II, Rigaku). The sample morphology was observed by SEM (JSM-6510, JEOL). The UV spectra were recorded (Lambda 750, PerkinElmer). The *J*-*V* photovoltaic measurements of the solar cells were carried out by employing an AM 1.5 solar simulator equipped with a xenon lamp (YSS-100A, Yamashita Denso). The power of the simulated light was calibrated to 1000 W/m<sup>2</sup> by using a reference Si photodiode (Bunkou Keiki, Japan).

### 3. Results and discussion

#### 3.1. CZTS precursor powder

Figure 3(a) shows the morphology of the CZTS precursor powder obtained after the ball-milling process at (800 rpm, 1 h). The particle size of the powder is about 50–500 nm. Some small particles agglomerated into big ones or clusters with diameter around 1–2  $\mu\text{m}$ .

A typical XRD pattern of the precursor powder is shown in Fig. 4(a). The diffraction peaks at  $28.93^\circ$ ,  $33.44^\circ$ ,  $47.68^\circ$ ,  $56.70^\circ$ , and  $77^\circ$  are correspondingly assigned to CZTS (112), (200), (220), (312), and (332) (PCPDF #260575). However, compared with the

standard PCPDF positions (see Fig. 4(a)), all of these diffraction peaks obviously shift by larger  $2\theta$  angles (about  $0.4^\circ$ ). The XRD peak shift phenomenon was not reported in Ref. [19] where the CZTS precursor powder was synthesized by a wet ball-milling process. In our study, the CZTS precursor powder is synthesized by a dry ball-milling process, so the interfacial area between the particles of the raw metal powders is smaller, and hence the rate of reaction is lower. The XRD peak shift may be caused by the stresses or the faults from the incomplete reaction.<sup>[32,33]</sup> From the XRD pattern of the precursor powder, we can see that the single phase CZTS precursor powder with preferred (112) orientation can be obtained by a simple mechanochemical ball-milling process.

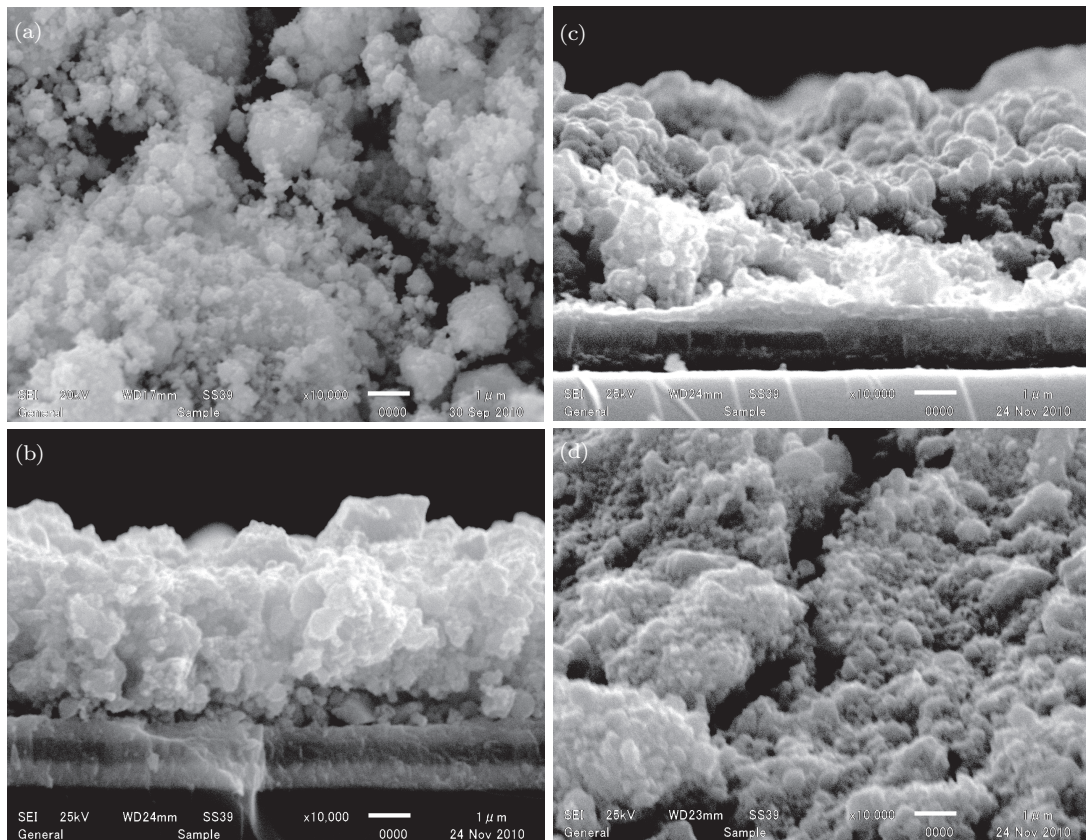


**Fig. 3.** SEM (a) image of CZTS precursor powder, (b) cross-section image of as-deposited CZTS film, (c) cross-section image of CZTS film annealed at  $600^\circ\text{C}$  for 9 min, and (d) surface image of CZTS film annealed at  $600^\circ\text{C}$  for 11 min.

#### 3.2. Annealing effects

##### 3.2.1. XRD analysis

To confirm the crystallinity and the phase composition of the CZTS film, XRD measurements were performed. Figure 4(a) depicts the XRD patterns of the CZTS films prepared at various annealing temperatures. The XRD patterns show clear peak

shift phenomena between the CZTS precursor powder and the heat-treated samples. The heat treatment, even the low-temperature heat treatment in air at  $125^\circ\text{C}$  for 5 min (the as-deposited sample), can retrieve the red shifted XRD peaks back to their usual positions (the PCPDF positions, see Fig. 4(a)), indicating that the peak shift can be easily improved. The diffraction peaks of the as-

deposited sample are still relatively weak and broad compared with that of the CZTS precursor powder. However, the XRD peaks of the annealed samples become sharp and strong compared with those of the as-deposited sample or the CZTS precursor powder. The sharp and strong peaks can be attributed to the improved crystallinity of the CZTS by the annealing process. As observed in Fig. 4(a), the peak intensity (especially (112)) increases as the annealing temperature is increased from 400 °C to 600 °C. Therefore, we choose 600 °C as the annealing temperature in the following experiments (the tolerable

temperature of the glass substrate is around 600 °C), because it can significantly improve the crystallinity of the CZTS.

Figure 4(b) shows the XRD patterns of the CZTS films annealed at 600 °C for various durations. The XRD peak intensity is strongly dependent on the annealing duration. The peak intensity increases as the annealing duration increases, and reaches its maximum when the annealing duration is 5 min. However, the peak intensity (especially (112)) distinctly decreases when the annealing duration is further increased to 7 min. It was reported that the evaporation of SnS and S from the CZTS easily occurred in high-temperature annealing process even without deliberately adding SnS and S.<sup>[34–36]</sup> Therefore, we speculate that the deterioration of the XRD peak may be due to the losses of Sn and S atoms from the CZTS after a long duration of annealing at high temperature under the N<sub>2</sub> ambient. Moreover, the XRD patterns (Fig. 4(c)) of the samples with long-time annealings, such as 9 min and 11 min, exhibit several new peaks (at 26.5°, 33.8°, and 51.7°) that do not belong to the CZTS. This indicates that the overlong annealing could result in a significant phase decomposition of the CZTS, which will seriously deteriorate the photovoltaic properties of the solar cell. Therefore, for the CZTS film, the annealing condition of (600 °C, 5 min) could be the optimal condition.

### 3.2.2. UV analysis

In order to investigate the annealing effects on the optical properties of the doctor-bladed CZTS films, we measured the UV absorption spectra of the samples annealed under different conditions. As shown in Fig. 5, the as-deposited film does not show any clear absorption edge possibly because of the amorphous nature of the film, whereas all the annealed samples show clear absorption edges. This indicates that the crystallinity of the CZTS can be improved by the annealing process. Interestingly, in the long wavelength range ( $\geq 894.7$  nm), the light absorption of the samples annealed at (600 °C, > 1 min) is rather high. This may be due to the existence of defects resulting from the phase decomposition of the CZTS (detailed analysis can be found in Subsection 3.2.1) in the high-temperature annealed films.

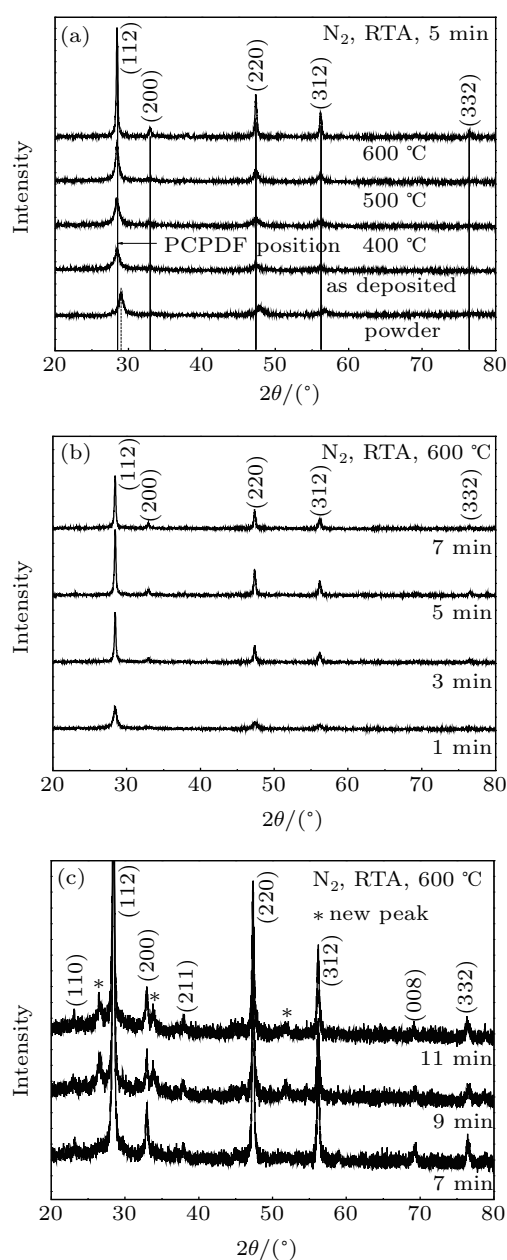


**Fig. 4.** XRD patterns of CZTS films annealed in N<sub>2</sub> ambient (a) at various temperatures and ((b) and (c)) for various durations.

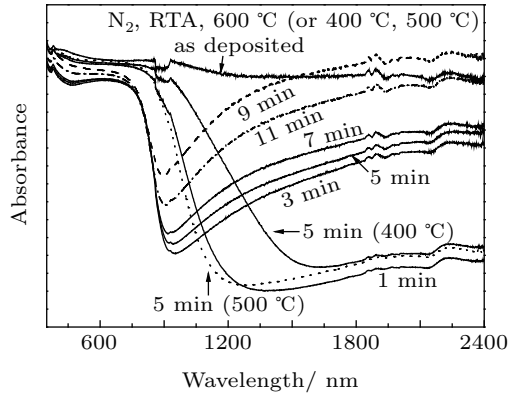


**Fig. 5.** UV absorption spectra of CZTS films annealed under different conditions.

In addition, from the absorption cutoff wavelengths, the calculated band gaps of the samples annealed at (400 °C, 5 min), (500 °C, 5 min), (600 °C, 1 min), (600 °C, 3 min), (600 °C, 5 min), (600 °C, 7 min), (600 °C, 9 min), and (600 °C, 11 min) are 0.846 eV, 1.138 eV, 1.076 eV, 1.386 eV, 1.394 eV, 1.406 eV, 1.418 eV, and 1.414 eV, respectively. The band gap generally increases as the annealing temperature and/or the annealing duration increases. However, it seems that the band gaps of the samples annealed at (600 °C,  $\geq 3$  min) are approximately a constant of 1.41 eV.

### 3.2.3. SEM analysis

The SEM images of the as-deposited and the annealed CZTS films (600 °C, 9 min and 11 min) are depicted in Fig. 3.

Figure 3(b) shows the cross-section image of the as-deposited CZTS film. The particle morphology and the size of the as-deposited CZTS film are similar to those of the precursor powder (Fig. 3(a)). The morphologies of the samples annealed at 600 °C for 1 min, 3 min, 5 min, and 7 min were also observed (data not shown). The result indicates that the morphologies of these annealed samples are all similar to those of the as-deposited CZTS film, although their crystallinities and optical properties have obviously changed as shown in the XRD and the UV data. Figure 3(c) shows the morphology of the sample annealed at (600 °C, 9 min). From the figure, significant material loss is observed, which may be due to the evaporation of materials from the phase decomposition of the CZTS as discussed in the XRD and the UV data. Moreover, many large cracks (Fig. 4(d)) appear on the film surface as the annealing duration is further increased to 11 min. As a result, the annealing duration for the CZTS film should be less than 9 min.

### 3.2.4. $J$ - $V$ analysis

In order to analyse the photoelectric properties of the doctor-bladed CZTS films, complete solar cells with the superstrate structure of FTO glass/TiO<sub>2</sub>/In<sub>2</sub>S<sub>3</sub>/CZTS/Mo were fabricated. Figure 6 shows the  $J$ - $V$  characteristics of the samples annealed at 600 °C for various annealing durations. The relevant parameters of the solar cells are listed in Table 1.

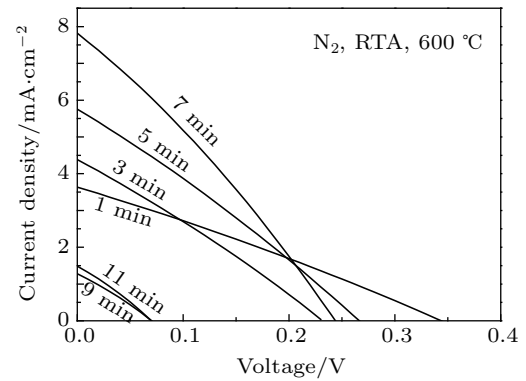


**Fig. 6.** The  $J$ - $V$  characteristics of CZTS absorption layers annealed at 600 °C for various durations.

**Table 1.** Solar cell parameters extracted from Fig. 6.

Annealing duration/min	$J_{sc}$ /mA·cm <sup>-2</sup>	$V_{oc}$ /V	FF	Efficiency /%
1	3.64	0.34	0.27	0.34
3	4.38	0.23	0.28	0.28
5	5.76	0.27	0.28	0.42
7	7.82	0.24	0.29	0.55
9	1.28	0.07	0.28	0.03
11	1.48	0.07	0.29	0.03

As shown in Fig. 6, the short current density ( $J_{sc}$ ) of the solar cell increases as the annealing duration increases from 1 min to 7 min. However, it significantly decreases as the annealing duration is further increased to 9 min and 11 min. This may be caused by the phase decomposition of the CZTS discussed. As shown in Table 1, the short-circuit current density ( $J_{sc}$ ), the open-circuit voltage ( $V_{oc}$ ), the fill factor (FF), and the efficiency of the best solar cell are 7.82 mA/cm<sup>2</sup>, 240 mV, 0.29, and 0.55%, respectively. The annealing duration for this solar cell is 7 min, which is longer than that deduced from the XRD result (figure 4(b) shows that the optimal annealing duration for the CZTS film should be 5 min). We explain the prolonged annealing duration as follows. For the XRD measurements, the used CZTS films were prepared on glass substrates, while for the solar cell, the

used CZTS absorption layers were deposited on the sulfur-rich  $\text{In}_2\text{S}_3$  buffer layer (details can be found in Subsection 2.2.1). During the annealing process, the sulfur-rich  $\text{In}_2\text{S}_3$  buffer layer could make a weak sulfur ambient, which could help suppress the element evaporation of the CZTS absorber layer and thus prolong the optimal annealing duration.

## 4. Conclusion

The results from the current study are as follows. (i) The XRD peaks of the CZTS precursor powder synthesized by the dry ball-milling process show clear red shift phenomena. (ii) The annealing parameters, including the sulfur-rich  $\text{In}_2\text{S}_3$  buffer layer, have strong effects on the structural, the optical, and the morphological properties of the doctor-bladed CZTS film. Notably, annealings can also introduce defects into the CZTS film. (iii) The short-circuit current density, the open-circuit voltage, the fill factor, and the efficiency of the best solar cell are  $7.82 \text{ mA/cm}^2$ ,  $240 \text{ mV}$ ,  $0.29$ , and  $0.55\%$ , respectively. (iv) The particle size of the ball-milling synthesized CZTS precursor powder is rather big, which has a high melting point and hence significantly restricts the quality improvement of the solar cell absorption layer. The investigation for improving the solar cell conversion efficiency, such as the synthesis of low melting point CZTS nanoparticles, is under way.

## References

- [1] Li T, Zhou C L, Song Y, Yang H F, Gao Z H, Duan Y, Li Y Z, Liu Z G and Wang W J 2011 *Acta Phys. Sin.* **60** 098801 (in Chinese)
- [2] Han T, Meng F Y, Zhang S, Wang J Q and Cheng X M 2011 *Acta Phys. Sin.* **60** 027303 (in Chinese)
- [3] Yu H Z and Wen Y X 2011 *Acta Phys. Sin.* **60** 785 (in Chinese)
- [4] Li G L, Huang Z Y, Li K, Zhen H Y, Shen W D and Liu X 2011 *Acta Phys. Sin.* **60** 077207 (in Chinese)
- [5] Zhang L, He Q, Xu C M, Xue Y M, Li C J and Sun Y 2008 *Chin. Phys. B* **17** 3138
- [6] Xu C M, Sun Y, Li F Y, Zhang L, Xue Y M, He Q and Liu H T 2007 *Chin. Phys.* **16** 788
- [7] Li W, Sun Y, Liu W, Li F Y and Zhou L 2006 *Chin. Phys.* **15** 878
- [8] Katagiri H, Jimbo K, Maw W S, Oishi K, Yamazaki M, Araki H and Takeuchi A 2009 *Thin Solid Films* **517** 2455
- [9] Katagiri H, Saitoh K, Washio T, Shinohara H, Kurumadani T and Miyajima S 2001 *Sol. Energy Mater. Sol. Cells* **65** 141
- [10] Katagiri H 2005 *Thin Solid Films* **480–481** 426
- [11] Liu F, Li Y, Zhang K, Wang B, Yan C, Lai Y, Zhang Z, Li J and Liu Y 2010 *Sol. Energy Mater. Sol. Cells* **94** 2431
- [12] Volobujeva O, Raudoja J, Mellikov E, Grossberg M, Bereznev S and Traksmaa R 2009 *J. Phys. Chem. Solids* **70** 567
- [13] Wibowo R A, Kim W S, Lee E S, Munir B and Kim K H 2007 *J. Phys. Chem. Solids* **68** 1908
- [14] Seola J S, Lee S Y, Lee J C, Nam H and Kim K 2003 *Sol. Energy Mater. Sol. Cells* **75** 155
- [15] Redinger A and Siebentritt S 2010 *Appl. Phys. Lett.* **97** 092111
- [16] Zhang K, Liu F Y, Lai Y Q, Li Y, Yan C, Zhang Z A, Li J and Liu Y X 2011 *Acta Phys. Sin.* **60** 028802 (in Chinese)
- [17] Todorov T K, Reuter K B and Mitzi D B 2010 *Adv. Mater.* **22** 156
- [18] Tanaka K, Oonuki M, Moritake N and Uchiki H 2009 *Sol. Energy Mater. Sol. Cells* **93** 583
- [19] Zhou Z, Wang Y, Xu D and Zhang Y 2010 *Sol. Energy Mater. Sol. Cells* **94** 2042
- [20] Tanaka K, Moritake N and Uchiki H 2007 *Sol. Energy Mater. Sol. Cells* **91** 1199
- [21] Miyamoto Y, Tanaka K, Oonuki M, Moritake N and Uchiki H 2008 *Jpn. J. Appl. Phys.* **1** 596
- [22] Todorov T K, Kita M, Carda J and Escibano P 2009 *Thin Solid Films* **517** 2541
- [23] Moritake N, Fukui Y, Oonuki M, Tanaka K and Uchiki H 2009 *Phys. Status Solidi (c)* **6** 1233
- [24] Tanaka K, Moritake N, Oonuki M and Uchiki H 2008 *Jpn. J. Appl. Phys.* **47** 598
- [25] Kamoun N, Bouzouita H and Rezig B 2007 *Thin Solid Films* **515** 5949
- [26] Kumar Y B K, Babu G S, Bhaskar P U and Raja V S 2009 *Phys. Status Solidi (a)* **206** 1525
- [27] Chan C P, Lam H and Surya C 2010 *Sol. Energy Mater. Sol. Cells* **94** 207
- [28] Wada T, Matsuo Y, Nomura S, Miyamura A, Chiba Y, Yamada A and Konagai M 2006 *Phys. Status Solidi (a)* **203** 2593
- [29] Chiba Y, Yamada A, Konagai M, Matsuo Y and Wada T 2008 *Jpn. J. Appl. Phys.* **47** 694
- [30] Kavan L and Gratzel M 1995 *Electrochim. Acta* **40** 643
- [31] John T T, Bini S, Kashiwaba Y, Abe T, Yasuhiro Y, Kartha C S and Vijayakumar K P 2003 *Semicond. Sci. Technol.* **18** 491
- [32] Ungar T 2004 *Scripta Mater.* **51** 777
- [33] Feng J, Yeung K K, Wong K W, Fu Eric C L and Lam C C 2000 *Supercond. Sci. Technol.* **13** 215
- [34] Scragg J J, Ericson T, Kubart T, Edoff M and Platzer-Bjorkman C 2011 *Chem. Mater.* **23** 4625
- [35] Weber A, Mainz R and Schock H W 2010 *J. Appl. Phys.* **107** 013516
- [36] Redinger A, Berg D M, Dale P J and Siebentritt S 2011 *J. Am. Chem. Soc.* **133** 3320